Supplement of Atmos. Chem. Phys., 21, 8961–8977, 2021
https://doi.org/10.5194/acp-21-8961-2021-supplement

Atmospheric Chemistry and Physics
Open Access
EGU

Supplement of

Measurement report: Molecular composition and volatility of gaseous organic compounds in a boreal forest – from volatile organic compounds to highly oxygenated organic molecules

Wei Huang et al.

Correspondence to: Wei Huang (wei.huang@helsinki.fi) and Federico Bianchi (federico.bianchi@helsinki.fi)

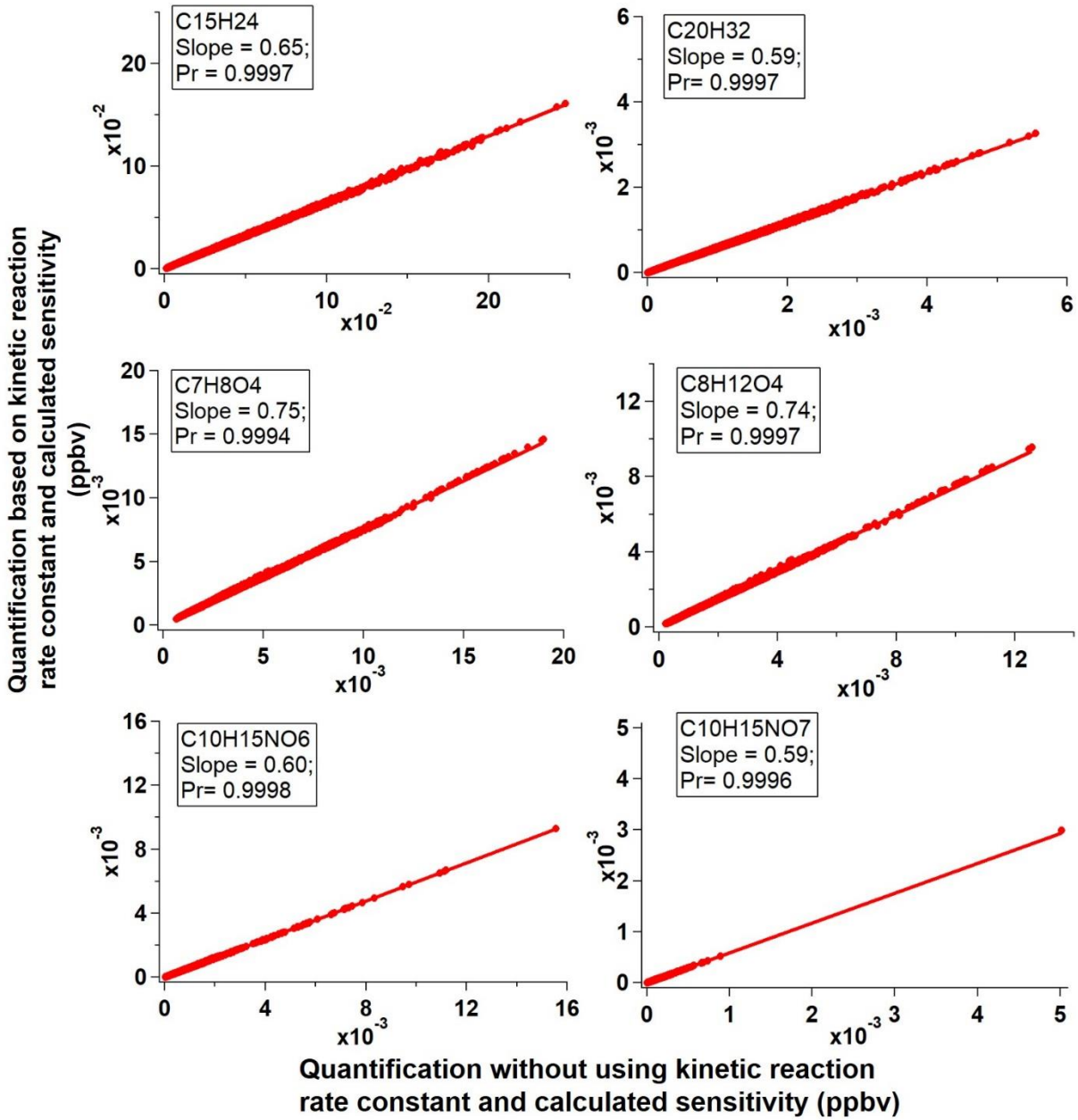

Figure S1. Comparison for the Vocus quantification based on the kinetic reaction rate constant and calculated sensitivity (Sekimoto et al., 2017; Yuan et al., 2017) vs. the Vocus quantification without using it.

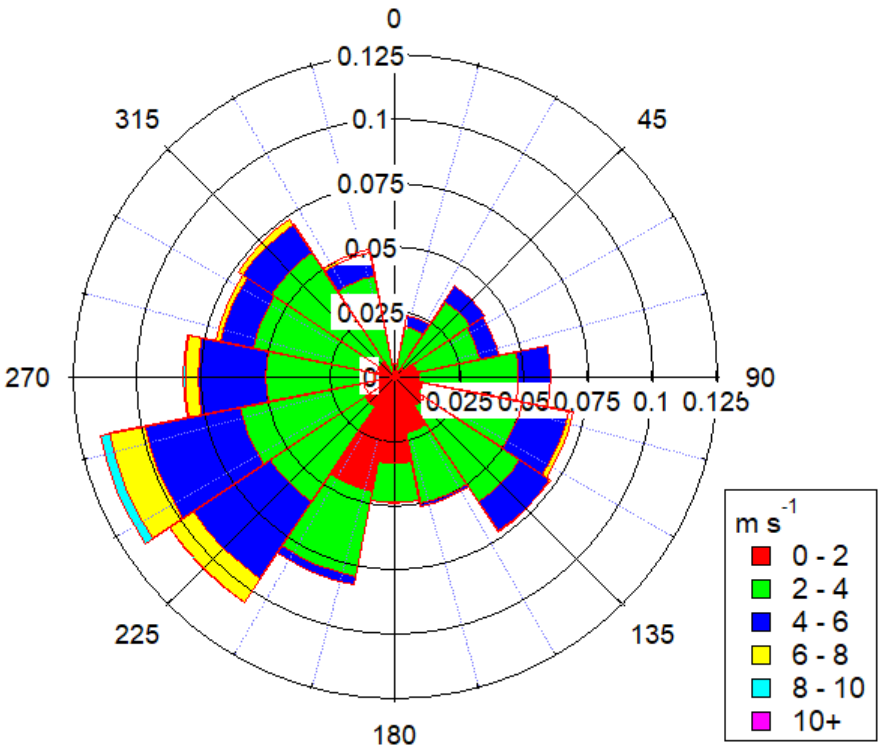

Figure S2. Wind speeds and directions during the measurement period.

Table S1. Full list of relatively long-lived species excluded from Vocus data present in this study.

Detected ion	Potential name
$C_2H_7O^+$	Ethanol
$C_3H_7O^+$	Acetone
$C_2H_5O_2^+$	Acetic acid
$C_2H_5O_3^+$	Glycolic acid
$C_3H_9O_2^+$	Acetone with water cluster

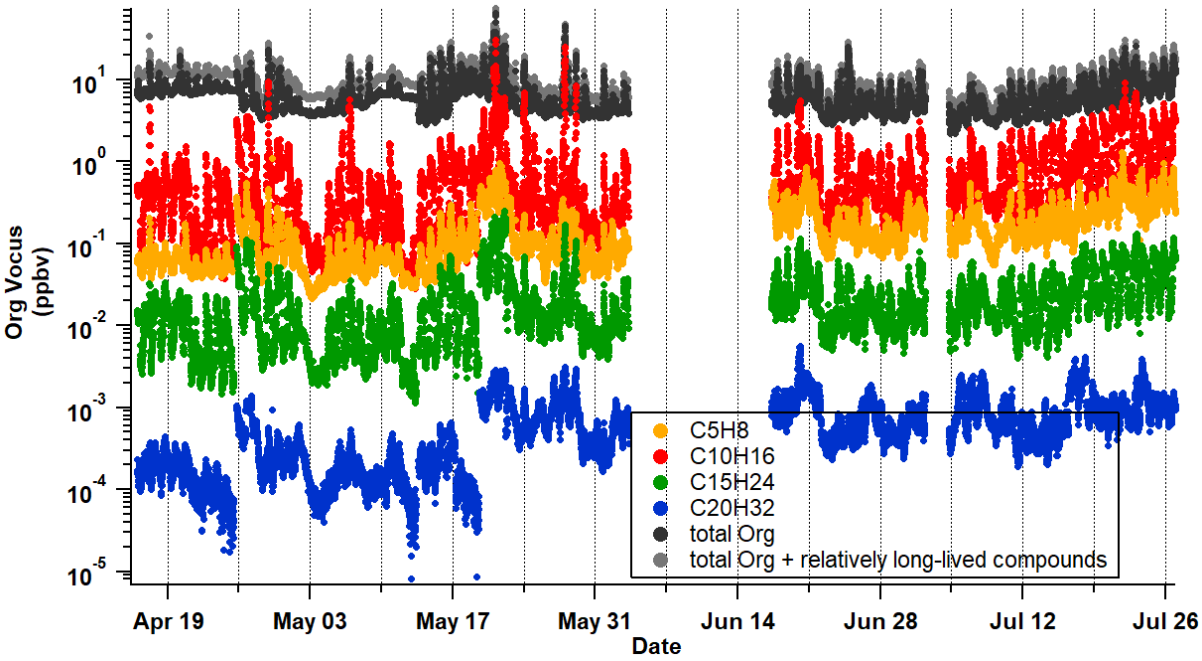

Figure S3. Time series of terpenes (isoprene, monoterpenes, sesquiterpenes, and diterpenes), all organic compounds (for comparison, same as in Fig. 1f), and all organic compounds + relatively long-lived compounds measured by Vocus.

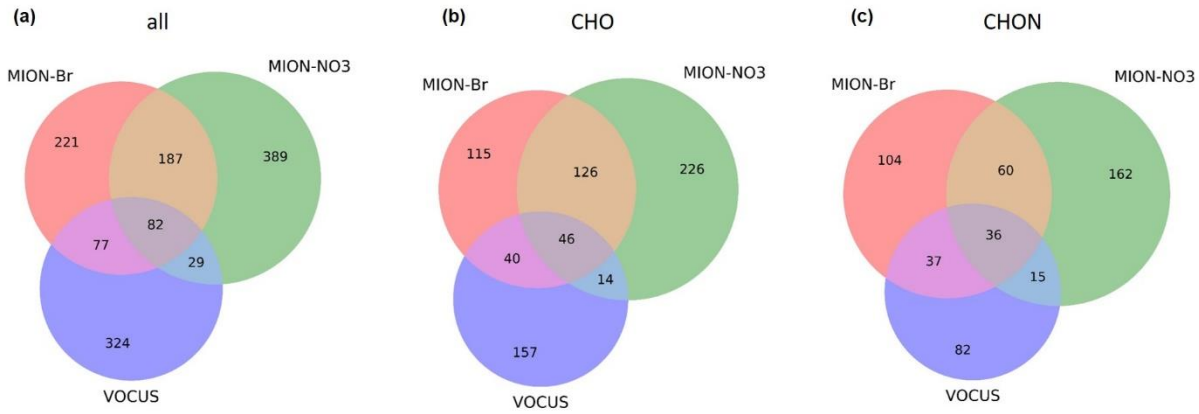

Figure S4. Overlaps of all organic compounds **(a)**, CHO compounds **(b)**, and CHON compounds **(c)** measured by Vocus, MION-Br, and MION-NO_3.

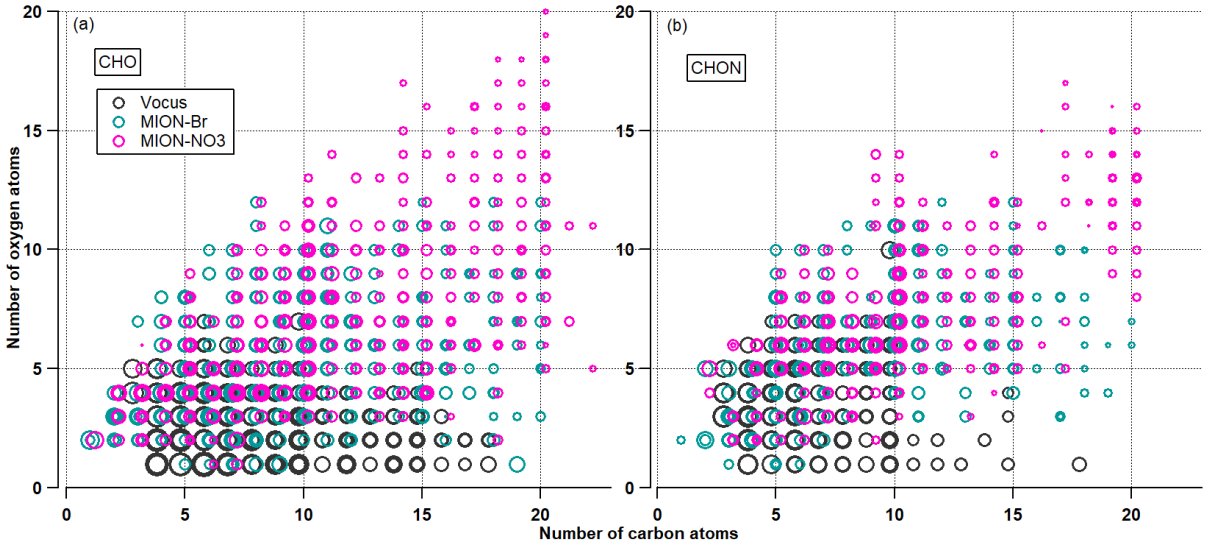

Figure S5. Distribution of CHO compounds **(a)** and CHON compounds **(b)** measured by Vocus, MION-Br, and MION-NO_3 as a function of number of oxygen atoms vs. number of carbon atoms. Markers were sized by the logarithm of their corresponding concentrations.

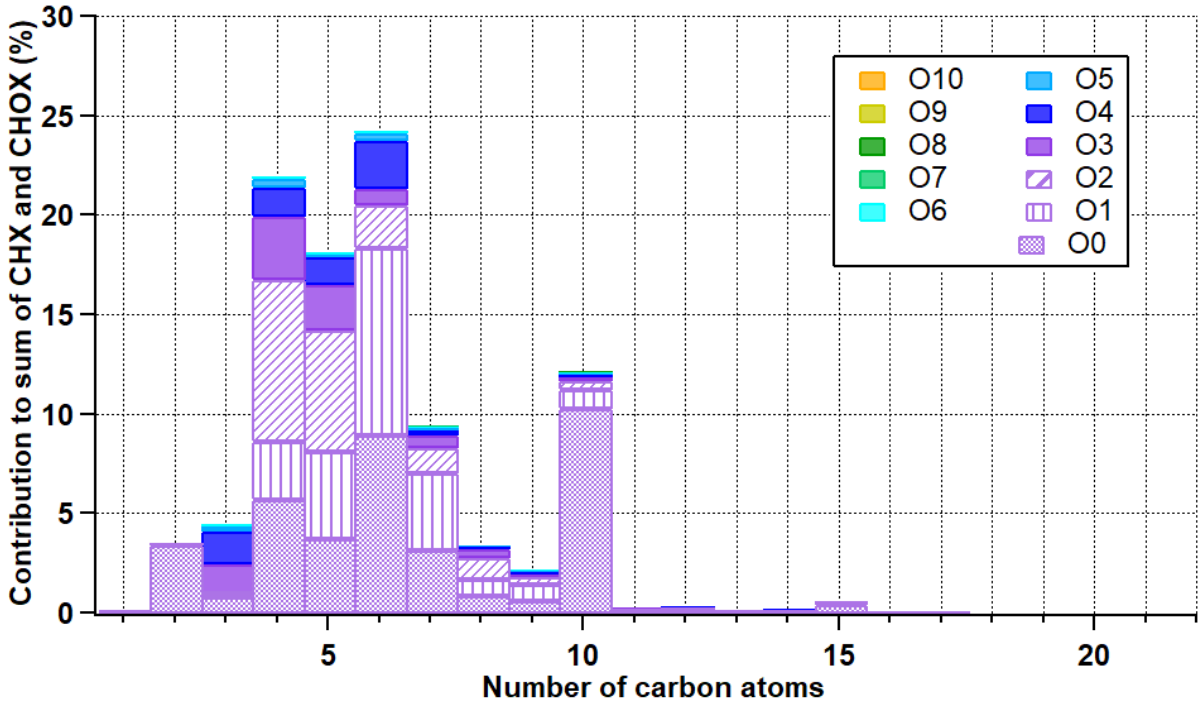

Figure S6. Contribution of organic compounds with different number of oxygen atoms to all organic compounds (including CHX compounds) as a function of the number of carbon atoms measured by Vocus.

Table S2. Sum contribution (%, average ± 1 standard deviation) of C_xH, C_xHO, and C_xHON groups (x = 5, 10, 15, and 20) to total CH, CHO and CHON compounds measured by different measurement techniques.

Compound group	Vocus	MION-Br	MION-NO_3
C_xH/CH	38.3 ± 12.5 %	-	-
C_xHO/CHO	27.4 ± 3.2 %	20.0 ± 4.4 %	26.8 ± 5.7 %
C_xHON/CHON	16.2 ± 2.3 %	34.9 ± 4.2 %	38.6 ± 4.5 %

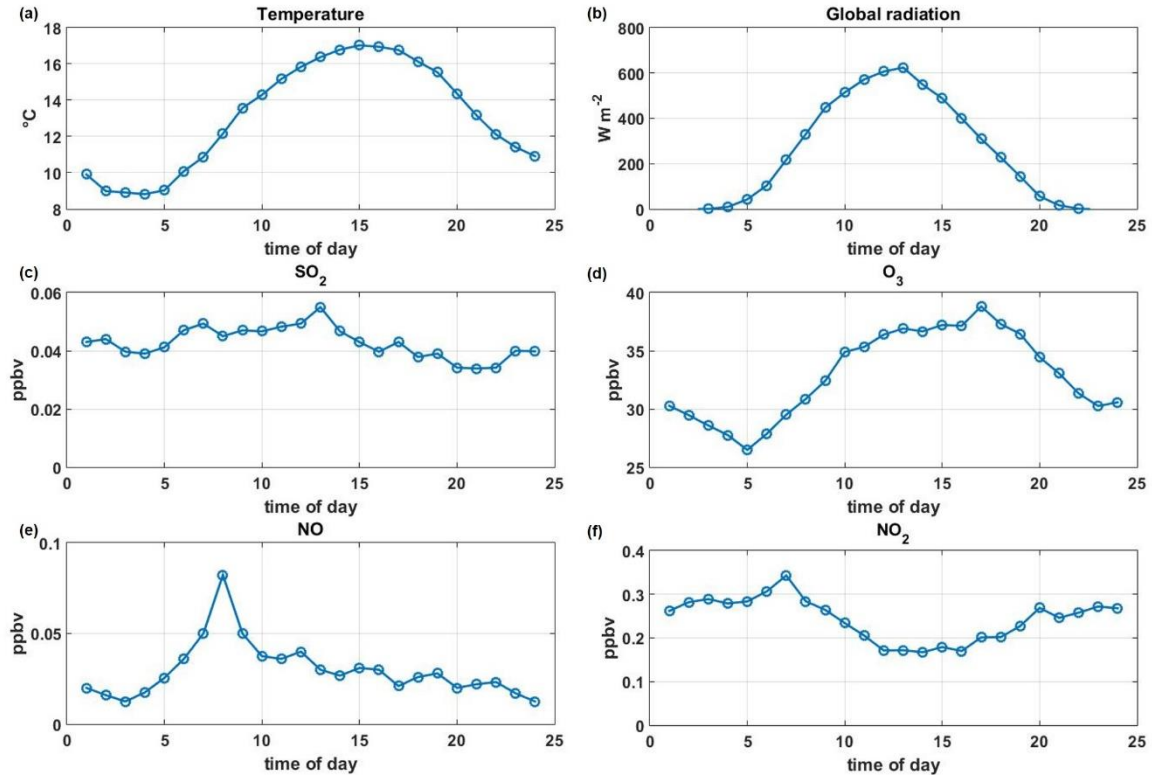

Figure S7. The median diurnal patterns of temperature **(a)**, global radiation **(b)**, mixing ratios of SO_2 **(c)**, O_3 **(d)**, NO **(e)**, and NO_2 **(f)** during the measurement period.

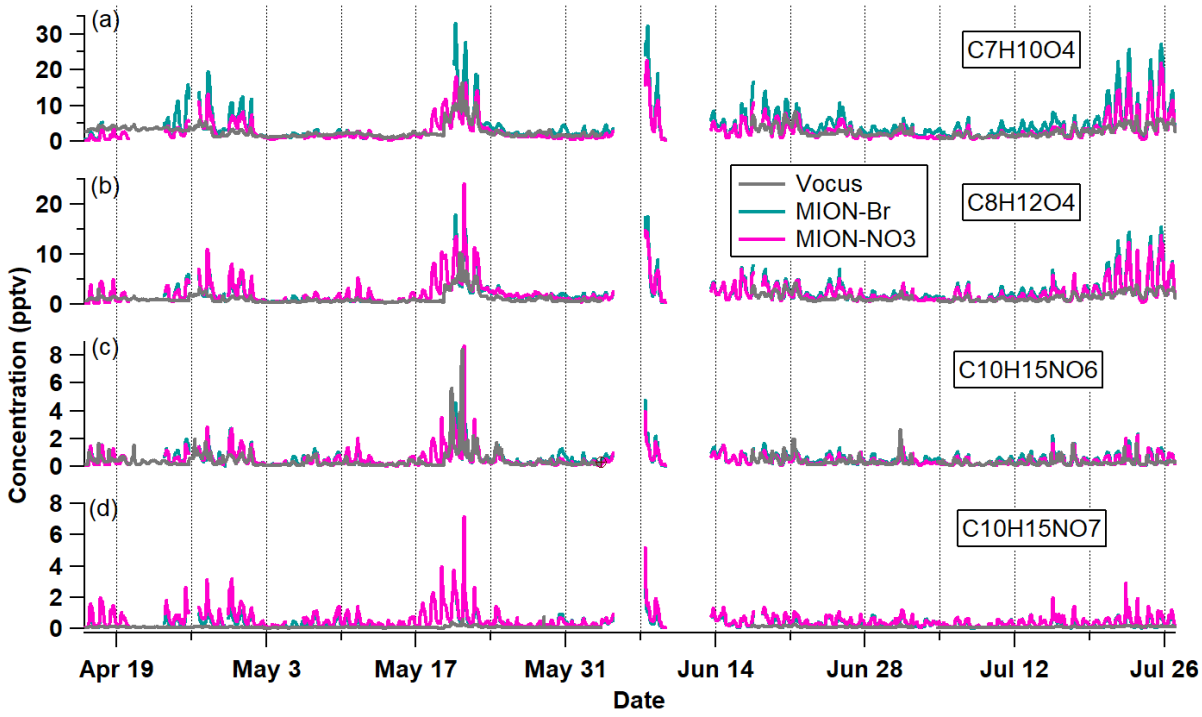

Figure S8. Time series of the dominant CHO and CHON species measured by Vocus, MION-Br, and MION-NO_3.

Table S3. Pearson's R correlations for dominant CHO and CHON species among different measurement techniques.

Compound	Vocus vs. MION-Br	Vocus vs. MION-NO_3	MION-Br vs. MION-NO_3
$C_7H_{10}O_4$	0.63	0.65	0.96
$C_8H_{12}O_4$	0.64	0.66	0.96
$C_{10}H_{15}NO_6$	0.35	0.36	0.93
$C_{10}H_{15}NO_7$	0.47	0.43	0.94

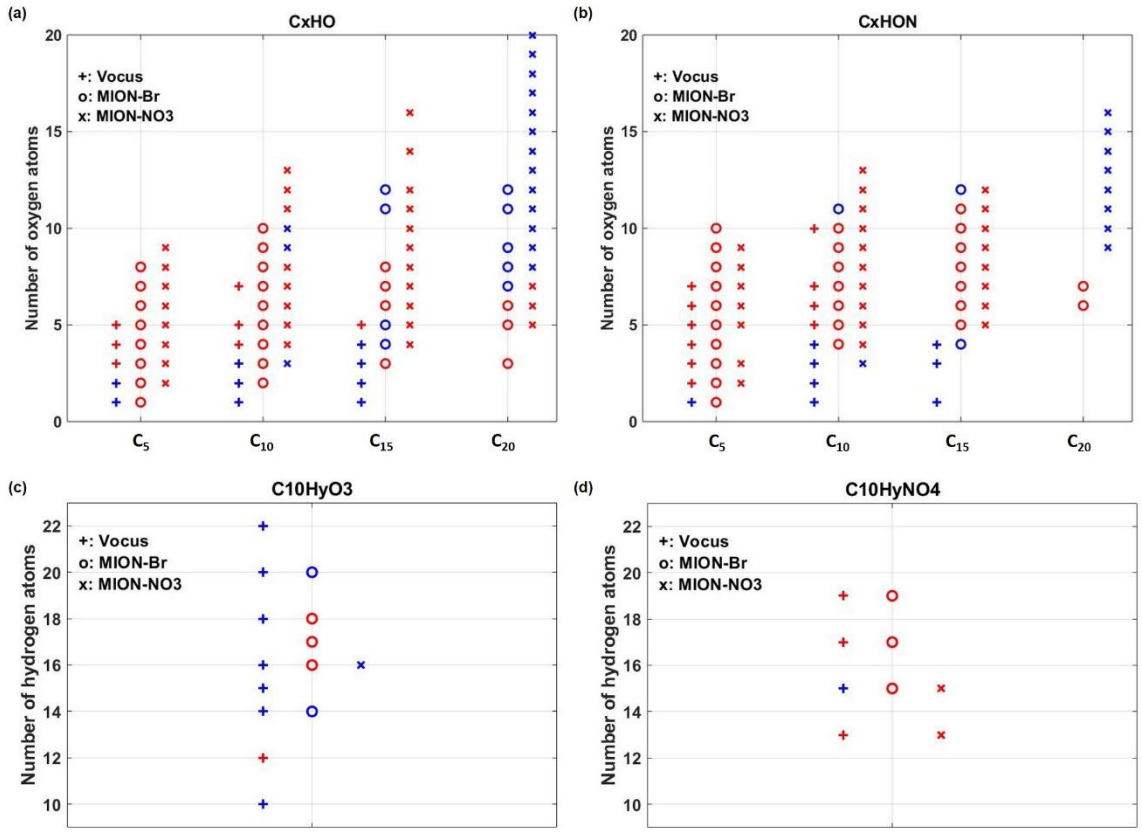

Figure S9. Comparison of the daytime (between 10:00 and 17:00) and nighttime (between 22:00 and 05:00) levels of C_xHO **(a)** and C_xHON **(b)** compounds (x = 5, 10, 15, 20) as a function of the number of oxygen atoms measured by Vocus (in pluses), MION-Br (in circles), and MION-NO_3 (in crosses); comparison of the daytime and nighttime levels of of $C_{10}H_yO_3$ **(c)** and $C_{10}H_yNO_4$ **(d)** as a function of the number of hydrogen atoms measured by Vocus (in pluses), MION-Br (in circles), and MION-NO_3 (in crosses). Compounds with higher signals during the daytime are colored in red and those with higher signals during the nighttime are colored in blue.

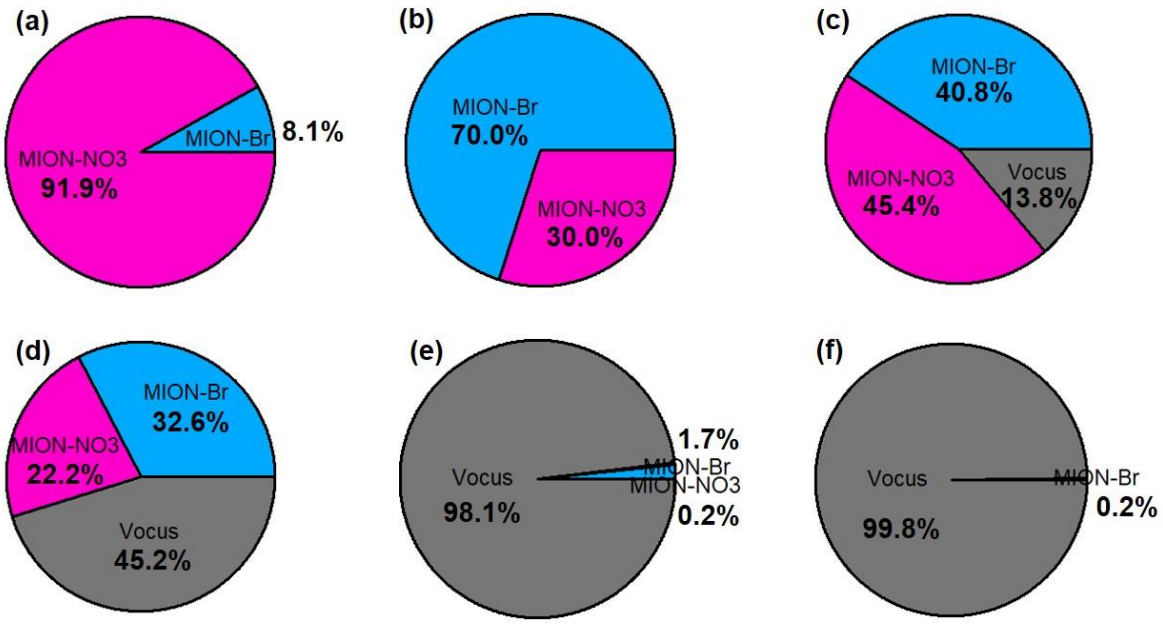

Figure S10. Fraction of ULVOC **(a)**, ELVOC **(b)**, LVOC **(c)**, SVOC **(d)**, IVOC **(e)**, and VOC **(f)** of all measured organic compounds (with the approach described in section 2.2.1) which were only detected by or highestly detected by Vocus, MION-Br, and MION-NO_3.

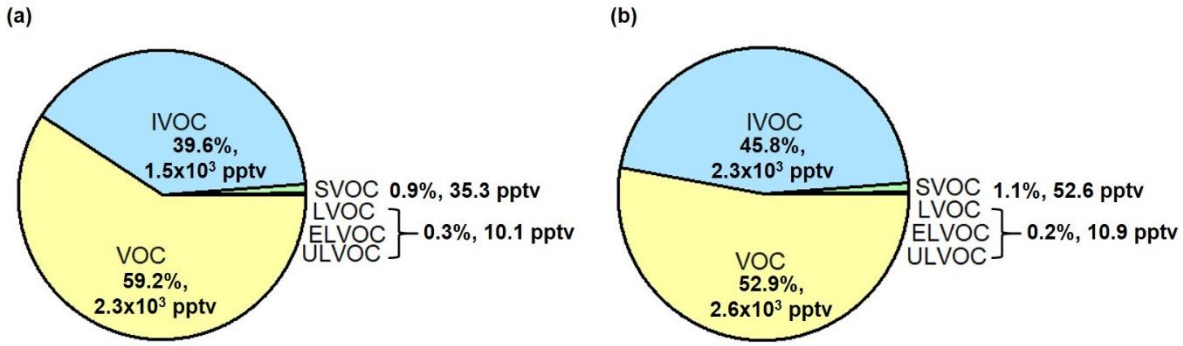

Figure S11. Pie charts for the contributions of VOC, IVOC, SVOC, LVOC, ELVOC, and ULVOC of all measured organic compounds (with the approach described in section 2.2.1) parameterized with the modified Li et al. (2016) approach (Daumit et al., 2013; Isaacman-VanWertz and Aumont, 2021) during the daytime **(a)** and nighttime **(b)**.

References

Li, Y., Pöschl, U., and Shiraiwa, M.: Molecular corridors and parameterizations of volatility in the chemical evolution of organic aerosols, Atmos Chem Phys, 16, 3327–3344, https://doi.org/10.5194/acp-16-3327-2016, 2016.

Daumit, K. E., Kessler, S. H., and Kroll, J. H.: Average chemical properties and potential formation pathways of highly oxidized organic aerosol, Faraday Discuss, 165, 181-202, https://doi.org/10.1039/C3FD00045A, 2013.

Isaacman-VanWertz, G., and Aumont, B.: Impact of organic molecular structure on the estimation of atmospherically relevant physicochemical parameters, Atmos Chem Phys, 21, 6541–6563, https://doi.org/10.5194/acp-21-6541-2021, 2021.

Sekimoto, K., Li, S. M., Yuan, B., Koss, A., Coggon, M., Warneke, C., and de Gouw, J.: Calculation of the sensitivity of proton-transfer-reaction mass spectrometry (PTR-MS) for organic trace gases using molecular properties, Int J Mass Spectrom, 421, 71–94, https://doi.org/10.1016/j.ijms.2017.04.006, 2017.

Yuan, B., Koss, A. R., Warneke, C., Coggon, M., Sekimoto, K., and de Gouw, J. A.: Proton-transfer-reaction mass spectrometry: applications in atmospheric sciences, Chem Rev, 117, 13187–13229, https://doi.org/10.1021/acs.chemrev.7b00325, 2017.